2010 IEEE International Conference on Robotics and Automation
Anchorage Convention District
May 3-8, 2010, Anchorage, Alaska, USA

Cardiac Interventions under MRI Guidance using Robotic Assistance

Ming Li*, Ankur Kapoor†, Dumitru Mazilu*, Bradford Wood†, and Keith A. Horvath*
*National Heart, Lung, and Blood Institute, National Institutes of Health, Bethesda, MD, USA
Email: {lim2, mazilud, horvathka}@mail.nih.gov
†Clinical Center, National Institutes of Health, Bethesda, MD, USA
Email: {kapooran, bwood}@mail.nih.gov

Abstract— **Transapical aortic valve replacement under MRI guidance in a beating heart is a recent minimally invasive technique that could benefit from a surgical assistant system. We present a robotic surgical assistant system that can precisely and repeatably deliver aortic valve prostheses. The surgical system consists of an imaging system, an Innomotion robotic arm, a 3-DoF valve delivery module and user interfaces. Interactive control allows the physician to remain in the loop and adjust the orientation and position using real-time MR feedback. The 3-DoF valve delivery module is developed to deploy both balloon-expandable and self-expanding stented prostheses. We use a new compact fiducial that can be placed close to the volume of interest and requires a single image plane for image based robot registration.**

We evaluate the MRI compatible valve delivery module for both types of prostheses. The accuracy for prosthesis delivery is about 0.8 mm and 1.5 mm, for self-expanding and balloon-expandable prostheses, respectively. Preliminary results in ex-vivo experimentation suggest that the robotic system can be translated into animal and clinical models.

I. Introduction

Transapical aortic valve replacement is a recently developed minimally invasive approach that allows placement of a prosthetic valve via the apex of the beating heart. Compared to the other imaging modalities used in this procedure, such as fluoroscopy/echocardiography [1], real-time magnetic resonance imaging [2] provides high resolution images of cardiovascular anatomy without contrast or radiation. Use of real-time MRI allows physicians to monitor the progress of the procedure and also provides the ability to immediately assess the results, such as ventricular and valvular function, and myocardial perfusion. Precise placement of the prosthesis in a beating heart inside an MRI scanner is a complicated task due to the limited space and awkward accessing angle. In the current manual procedure, it is hard to manipulate instruments precisely inside MRI bore. It also requires a coordinated effort between the surgeon and the assistant in the noisy MRI environment with the heart and lungs moving.

Our group is currently focusing on developing cardiac interventions under MRI guidance using robotic assistance [3], [4], [5]. In this paper, we present a redesigned robotic valve delivery module along with control components for our robotic assisted system. Interactive control allows the physician to remain in the loop and precisely adjust the final orientation and position of the prosthesis using real-time MR feedback. The robotic delivery module can deploy a self-expanding stented prosthesis, in addition to a balloon-expandable stented prosthesis. Thus, this module can benefit from the advantages of the self-expanding prosthesis as well. Image registration using a new compact fiducial that can be placed close to the volume of interest (VOI) and requires a single image plane is used to pre-position the delivery module to the pre-planned trajectory. In addition, to increase the intuitiveness of the robotic system to assist the surgeon in the cardiac intervention under MRI guidance, we employ a hands-on cooperative control [6] on the Innomotion robotic arm during preparatory phase of the procedure.

In a minimally invasive valve replacement, the bioprosthetic valve is mounted on a stent which is used to anchor the valve to the vessel or heart. A balloon-expandable stent has been used in the aortic valve replacement [1], [2]. The uncertainty of the stented prosthesis' orientation and position during the expanding of a balloon, may lead to the blockage of the coronary ostia. Self-expanding stents have been employed to eliminate the need for balloon expansion [7], [8]. The procedures using these two types of the prosthesis are slightly different. In a procedure using the balloon-expandable prosthesis, the distal end of the sheath of the loaded delivery device is placed below the aortic annulus level; pushing an inner rod will advance the crimped prosthesis out of the sheath to the desired position, and then the balloon will be inflated to deploy the prosthesis. In a procedure using the self-expanding prosthesis, the loaded delivery device will first go into the ascending aorta and the edge of the inner rod is placed at the aorta annulus level. The retraction of the sheath will let the crimped prosthesis expand and affix to the desired position. We redesigned the robotic module and its control support to deploy both prostheses.

As a device holder, the robot should be able to move the delivery device onto the planned trajectory. The precise positioning of the robotic device under image guidance requires the computation of the transformation for the robot coordinate frame to the scanner coordinate frame. Coil-based [9] and image-based registration [10], [11] are used in MRI-guided systems. Coil-based registration provides realtime data but is scanner dependent. Image-based registrations are scanner independent but are not real-time. We noticed that usually the fiducial used for image-based registrations are placed at some distance away from the tip of the interventional tool

or volume of interest [10], [11]. In the valve replacement procedure, a multi-channel body coil is used and volume that can be acquired with sufficient image quality is of limited size. Thus, a fiducial close to the VOI and image isocenter is preferred. Moreover, registration of the robot prior to the placing the patient on the table (and thus being able to place the fiducial at the isocenter) is not practical in this case, as preparatory procedure of inserting the trocar is preformed on the MRI table. We propose a compact fiducial pattern that can be integrated into the delivery device and placed close to the VOI for registration.

Contemporary researchers on medical MRI compatible robot have primarily focused on percutaneous biopsy, drug injection or radiotherapy seed implantation. Improving precision and accuracy, while maintaining compatibility and safety with MRI environment are the prime concerns for these systems [12], [13], [14]. These robotic systems make use of intra-operative images and a graphical user interface (GUI) to update the planned motions. Transapical aortic valve replacement is a multi-phase minimally invasive cardiac intervention. Pre-planned motion based on pre-operative images alone is not sufficient for the starting phase of a valve replacement procedure. We noticed that during the insertion of the delivery device into the trocar port, a cooperative control interface, similar to Johns Hopkins Steady-Hand surgical robot [15] and the systems developed by Davies' group [16] can provide the surgeon a more natural way to manipulate the robot.

In the next section, we provide a brief overview of the transapical aortic valve replacement procedure. In the sections that follow, we describe the main components, namely, the hands-on control, the registration methods and the valve delivery module.

II. Procedure Overview

The flow chart of the robotically-assisted transapical aortic valve replacement under MRI guidance is presented in figure 1. The surgical system consists of the imaging system, Innomotion robotic arm, valve delivery module and user interfaces. The imaging system provides standard MR sequences as well as a real-time interactive imaging sequence (rtMRI) [2]. The rtMRI provides feedback on the progress of the procedure, whereas, standard MR sequences are used for surgical planning and registration. The surgeon controls the robotic system via user interfaces. The robotic component consists of a 5-DoF Innomotion robotic arm and a 3-DoF valve delivery module. The Innomotion robotic arm is employed as the holder of the 3-DoF valve delivery module. The robotic arm maintains the delivery device such that its trajectory passes through the center of the aorta annulus. The compact robotic valve delivery module is designed for manipulating and placing the prosthesis into a beating heart inside MRI scanner.

The cardiac procedure has three distinct phases, namely, preparatory, pre-operative and intra-operative. In the preparatory phase, the subject undergoes a MRI scan for the surgeon to determine the aortic annular diameter, coronary ostial anatomy, and apical location. The surgeon performs preparatory procedures of placing the trocar into the apex of the heart. The Innomotion robotic arm is then mounted on the MRI table and adjusted such that its end-effector is close to the trocar port. The robotic valve delivery module is mounted on the Innomotion robotic arm. The surgeon uses cooperative hands-on interface to adjust the Innomotion robotic arm to insert the delivery device into the trocar. Once the delivery device is in place, the user input sensor is detached and the robotic arm is moved into the bore.

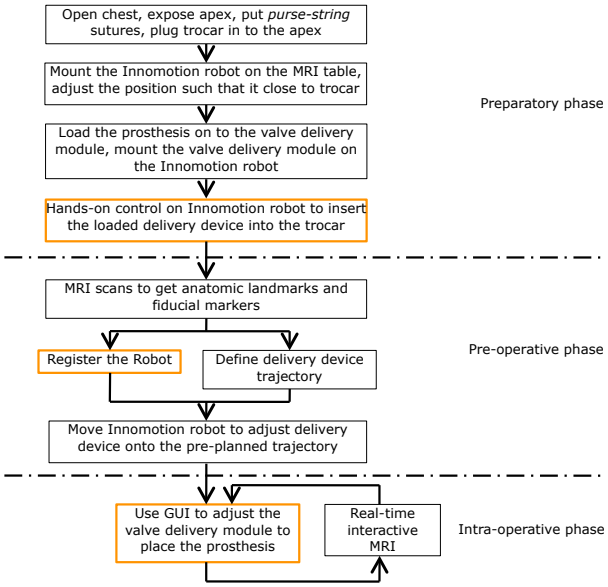

Fig. 1. Flow chart of robotically-assisted transapical aortic valve replacement under MRI guidance

In the pre-operative phase, the subject undergoes another MRI scan for the surgeon to plan the trajectory of the delivery device. At the same time, another MR sequence is used for registration. The Innomotion robotic arm is moved to the pre-planned trajectory, under image-guidance. Thus, direct access to the aortic valve is created.

In the intra-operative phase, the surgeon uses the visual feedback from the real-time interactive MR imaging to adjust the prosthesis. The surgeon can interactively adjust the prosthesis using the 3-DoF valve delivery module via a graphic user interface (GUI). Once the surgeon is satisfied with the prosthesis localization, he/she can use the GUI to deploy the prosthesis.

III. Methods

A. Hands-on Cooperative Control

We employ hands-on cooperative control on the pneumatically actuated robot [6] to directly insert the dexterous tool into the trocar during the preparatory phase. The robot acts like a laparoscopic tool holder similar to LARS [17], where the tool is an enhanced dexterous delivery device/module.

A key feature required for hands-on cooperative control of the robot is the ability to sense user input by using an

input device. We modified a commercially available 3D SpaceNavigator (3dconnexion, Fremont, CA) to be MR compatible, economic user input sensor. The 3D mouse uses a proprietary, advanced 6-DoF optical sensor [18]. The handle part of the sensor and its PC board is shielded with EMI/RFI shielding fabric. It can be attached and detached from the robot arm with a quick-detach mechanism. All the shields were either of aluminum or copper to avoid effects of the static magnetic field and grounded to the shielding of the room. We did not observe any noticeable difference in the sensor SNR when the sensor was brought up to 50 cm of the bore.

The low level controller gains of the pneumatically actuated robot were tuned such that fast and smooth response without oscillations was achieved during the transient as well as steady state. The high-level hands-on controller for the pneumatic robot was implemented using an optimization method for constrained control [19]. The desirable behavior here is that the robot continues to follow the user input as best as it can, even in the advent of certain limits, such as joint or velocity extremity.

B. Image-based Registration

Once the delivery device is inserted, the surgeon can take advantage of the precise positioning under image guidance. Registration is prerequisite for the image guidance. As shown in the figure 2(a), three elliptical grooves are carved around a 11 mm plastic rod. These 2.6 mm grooves are filled with diluted gadolinium (0.01 mol/L) and sealed. The length of the fiducial is 50 mm. The fiducial can be easily integrated into the distal end of the delivery device, and therefore can be placed inside the heart near the VOI and imaging isocenter while the patient is on the MRI table.

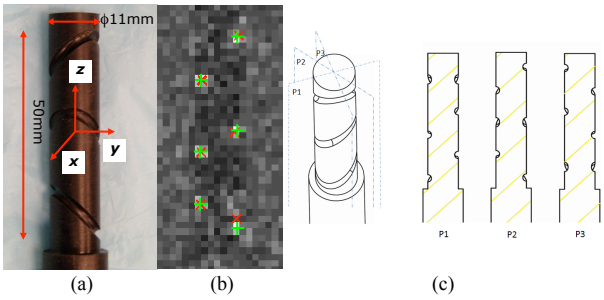

Fig. 2. (a) Fiducial with three elliptical patterns. (b) A MRI image passing through the center line of the fiducial, with segmented fiducial points. Red '×' are the intensity weighted centroids. Green '+' are final results of segmentation. (c) Sketch of the fiducial and 3 examples of cross-section of the fiducial.

The MRI sequence that we used for the registration is Siemens TrueFISP_IR, fast imaging with steady state precession with inverse recovery pulse using standard body coil. A good choice of parameter of inversion time will suppress both blood and myocardium signal. The parameters of the sequence we used for acquiring a bright signal of the fiducial in water is as follows: TR = 800 ms, TE = 2 ms, TI = 706 ms, flip angle = 50 deg, slice thickness = 1.05 mm, FOV = 188 × 287, and matrix = 126 × 192. The scan takes 26 s, which is tolerable within a breath hold. The image plane is chosen to pass through or nearly pass through the center line of the fiducial such that the image plane intersects with the three ellipses to obtain six bright fiducial points as shown in figure 2(b).

The first step in the registration process is the localization of these fiducial points in the image. We assume that each of these fiducials has a Gaussian intensity distribution, and use least-squares fitting techniques to obtain the parameters of the Gaussian that match each of the six fiducial points. The starting point for this optimization is obtained from the intensity weighted centroids of a threshold-filtered image. We have observed that the least-squares fit improves robustness especially in cases when the image points are non-circular due to partial volume effect and noise in the region of interest.

The next step is to determine the points in the fiducial coordinate frame corresponding to these image points [20]. Once the corresponding points are known, the transformation between the image coordinate frame and the fiducial coordinate frame, ${}^{f}\boldsymbol{T}_{i}$, can be obtained using point-to-point registration. Thus, theoretically only a single image plane is needed for registration.

The above mentioned MRI sequence provides a series of 10 slabs for each scan with 1.05 mm spacing. The central slabs are close to the center line of the fiducial, while the slabs towards two ends meet the edges of the fiducial. The image points on the central four to six slabs are circular and easily localized, while, those on the end slabs are elongated and more difficult to localize. Using all available slabs increases the robustness and accuracy of the registration.

The transformation from the scanner coordinate frame to the robot coordinate frame, ${}^{r}\boldsymbol{T}_{s}$, can be obtained by

$$ {}^{r}\boldsymbol{T}_{s} = {}^{r}\boldsymbol{T}_{f} \times {}^{f}\boldsymbol{T}_{i} \times ({}^{s}\boldsymbol{T}_{i})^{-1} \quad (1) $$

The transformation from the fiducial coordinate frame to the robot coordinate frame, ${}^{r}\boldsymbol{T}_{f}$, can be computed from the robot joint values and kinematics. The transformation from the image coordinate frame to the scanner coordinate frame, ${}^{s}\boldsymbol{T}_{i}$, can be read out from the DICOM header.

C. Valve Delivery Module

A MRI compatible 3-DoF valve delivery module was developed to provide precise and repeatable positioning of both balloon-expandable and self-expanding prostheses via a transapical approach. The prototype of the robotic module is shown in figure 3. The valve delivery module consists of two components: a sterilizable valve delivery unit and an active mechanism that provides the manipulation of the delivery device for a prosthetic valve placement. The valve delivery unit includes a delivery device, a trocar, and a trocar adaptor that is used for mounting the trocar on the active robotic mechanism. The robotic module was made from magnetic compatible materials and actuated with pneumatic actuators encoded with optical sensors. The active mechanism includes two linear joints - translation (A) and insertion (B) along with a rotational joint (C). The operations of linear and rotational

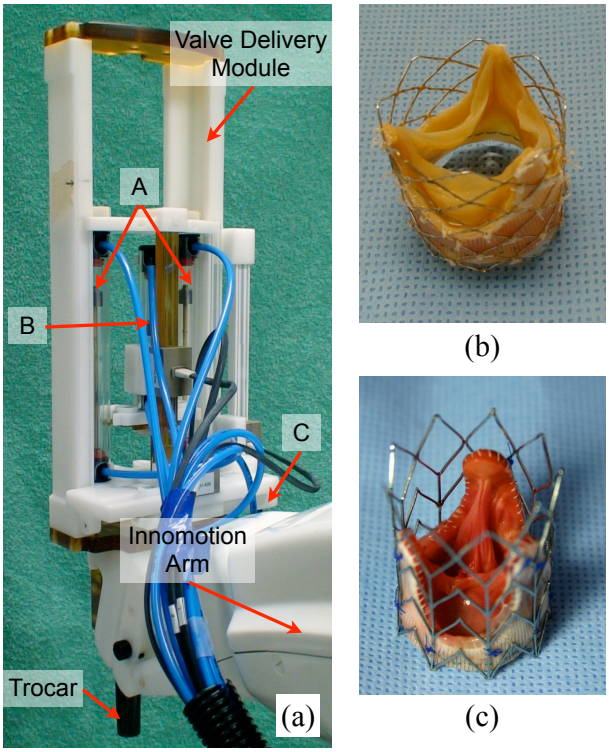

Fig. 3. (a) Prototype of the robotic valve delivery module (b) Balloon-expandable prosthesis (c) Self-expanding prosthesis

joints are independent. A PIV controller that runs on a DSP board was used for servoing the motion of the actuators.

The translation joint is directly actuated by two parallel linear pneumatic actuators. The two-actuator structure guarantees balanced motion of a delivery device. The bodies of two linear actuators, together with a base plate and a top plate form a rigid sliding frame. The sliding frame can slide on two frame rails. These two frame rails, along with a connecting plate and a top plate form a rigid frame. The connecting plate has grooves that match a corresponding adaptor on the last joint of the Innomotion robotic arm, which allows quick mounting/dismounting of the delivery module. The position is sensed by a linear optical encoder that is attached to one of the frame rails of the rigid frame. The insertion joint comprises of one central sliding stage with a semicircular groove actuated by a linear actuator that can slide on the rigid sliding frame. This linear movement is also encoded with a linear optical encoder. The rotational joint rotates the delivery device around its axis. This changes the orientation of the prosthesis relative to coronary ostia before it is deployed. It is actuated by a linear pneumatic actuator attached on the base plate of the sliding frame. The linear movement is transmitted to the rotational movement by a rack-gear transmission. A sliding base rack actuated by the pneumatic actuator transmits linear movement to the gears of the rotation joint. The rotation angle is sensed by a linear optical encoder.

The translation and insertion joints can be controlled independently or simultaneously. Sole motion of the translation joint moves the delivery device (both its inner rod and protecting sheath) back and forth. Sole motion of the insertion joint moves only the inner rod of the delivery device, driving the balloon-expandable prosthesis out of the protecting sheath to the desired position. Simultaneously retracting the translation joint and advancing the insertion joint at same velocity will keep the inner rod of the delivery device at its location and retract protecting sheath back to the inner rod. This simultaneous motion will let the crimped self-expanding prosthesis expand and affix to the desired position.

We implemented a continuous control mode (velocity mode), in addition to the previous existed point-to-point position move mode. With the continuous mode, the surgeon can start, stop or resume the joint motion any time he/she decides, therefore, he/she can monitor and control the progress during the prosthesis deployment. The continuous mode demands a smooth motion without oscillations during the transmission, i.e., the velocity error during the transmission should be small. The implementation of a continuous control mode on a pneumatic actuated joint is challenging, it requires the compromise between the smoothness, velocity and position error. Moreover, the insertion joint sits on the sliding frame that is actuated by the translation joint, thus, the two linear joints are coupled. The motion of one joint will effect the other one.

Typically, the distance between the aortic annulus and coronary ostia is about 9 mm, while the height of the lowest portion of the prosthesis is about 7 mm. To deploy a prosthesis at the optimal position, we targeted the accuracy of both the individual and combinative motion of linear joints as less than 2 mm.

IV. Experiments and Results

A. Registration

In this section we present the results of registration accuracy study. The purpose of the registration in our application is to command the robotic arm to adjust the delivery device to the pre-planned trajectory. The path of the pre-planned trajectory passes the apex, which usually is pre-located at the remote-center-of-motion of the Innomotion robot. Therefore, the rotation accuracy is more important in our case.

The fiducial was rigidly fixed to the Innomotion robot that was mounted on the MRI table. The fiducial was submerged under water. The robot was commanded to rotate around its remote-center-of-motion. The robot was first commanded to rotate and stop at 7 different poses in the *craniocaudal* direction and then in 7 different poses in the *axial* direction of the MRI scanner. We recorded the robot joint at each pose and calculated the relative angular values between any of two poses. These values served as the ground truth. We also scanned the fiducial at each pose and computed the rotation from the fiducial coordinate frame to the scanner coordinate frame, ${}^{s}\boldsymbol{T}_{f}$. We calculated the Euler angles between any of two poses based on the computed ${}^{s}\boldsymbol{T}_{f}$. The rotation errors based on 7 different poses in both directions are reported in table I. The transformation is also computed for the same set of poses using the markers provided along with the Innomotion

robot [17]. This marker consists of four spherical hollow balls ($\phi 15$ mm or $\phi 10$ mm) filled with MR contrast agent rigidly attached to the last joint of the Innomotion robot.

TABLE I

RELATIVE ERROR OF REGISTRATION FOR EACH DIRECTION (7 POSES IN EACH DIRECTION)

	Craniocaudal (deg)		Axial (deg)	
	Mean	Std. Dev.	Mean	Std. Dev.
Fiducial marker	0.62	0.50	0.36	0.30
Innomotion markers	0.63	0.72	0.36	0.33

B. Interactive Continuous Mode

We evaluated the smoothness, speed and error of two linear joints of the robotic valve delivery module under the continuous mode. The air pressure we used to actuate the pneumatic pistons was 75psi (520kPa). We moved the translation and insertion joints of the robot in the continuous mode and recorded their position and velocity using the encoders (resolution 2μm).

The position and velocity profile of two linear joints with velocity as 1 mm/s under the continuous mode are shown in figure 4. These errors are only from the motion of the valve delivery module. The maximum position error of the translation joint is less than 0.3 mm and its maximum velocity error is less than 0.2 mm/s. The maximum position error of the insertion joint is less than 0.5 mm and its maximum velocity error is less than 0.2 mm/s. During the self-expanding prosthesis deployment, which is a combined motion of translation and insertion joints, the maximum position error of the tip of the inner rod of the delivery device is less than 0.5 mm and its maximum position error rate is less than 0.5 mm/s.

C. Prosthesis Delivery

We also tested the accuracy and repeatability of the delivery module for both self-expanding and balloon-expandable prosthesis deployment. A phantom was designed to emulate the valve replacement situation. It consisted of a plastic tube with 25 mm diameter, which served as the aorta. The diameter of the tube is typical size of adult human aortic root. This was mounted on one side of a $200 \times 100 \times 100$ mm water tank. A spherical joint mounted on the opposite side of the tank served as the apex. A $12-15$ mm trocar was inserted into the spherical joint. The distance from spherical joint to the end of the plastic tube was 50 mm, which is the typical distance from the heart apex to the aorta annulus as measured in clinical scenario. The robotic valve delivery module was mounted such that the axis of the delivery device passes through the center of the tube end.

The delivery device was positioned using the GUI such that the distal end of the prosthesis was at the target mark on the tube. The GUI was then used to deploy the prosthesis. We measured the distance between the distal end of the prosthesis and the target mark using a caliper (resolution 0.01 mm). This error is cumulative error from robotic arm, the valve delivery module and the motion and/or slippage of the prosthesis during

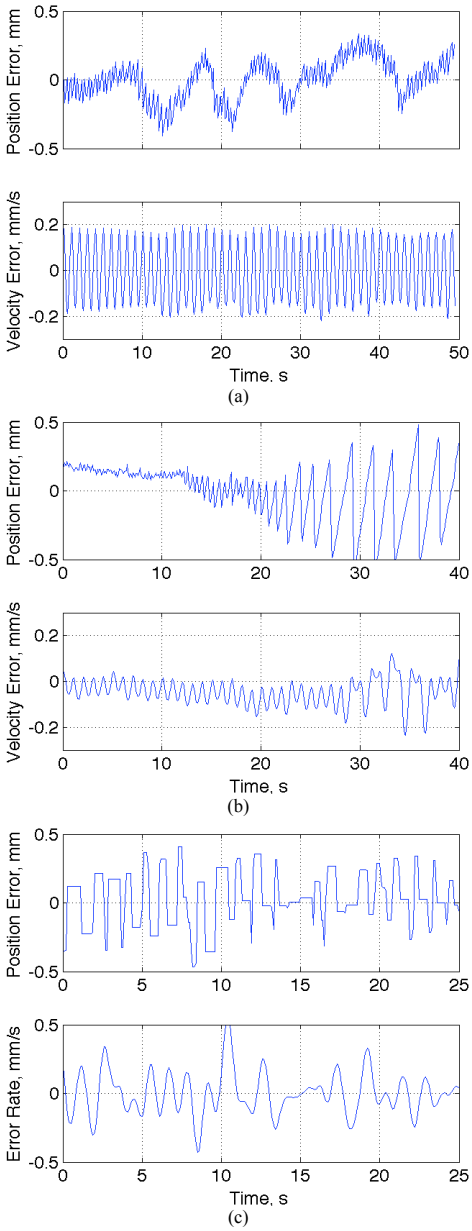

Fig. 4. Position and velocity error of (a) Translation joint, (b) Insertion joint, and position error and error rate of (c) Combination motion of translation and insertion joints to deploy self-expending prosthesis.

the deployment. The average distance and standard deviation for the self-expanding prosthesis based on nine trials and for balloon-expandable prosthesis based on eight trials are shown in table II. Figure 5 shows our setup and the progress of one of the trials with the self-expanding prosthesis.

TABLE II

POSITION ERROR FOR PROSTHESIS DELIVERY

	Self-Expanding	Balloon-Expandable
Mean	0.8 mm	1.5 mm
Std. Dev.	0.4 mm	0.2 mm

Our delivery module can deploy both the prosthesis with reasonable accuracy. The balloon-expandable prosthesis has a

slightly larger error because during the deployment there is a possibility that the prosthesis slides and rotates on the balloon. Moreover, the balloon may not expand uniformly, causing the prosthesis to move from its position.

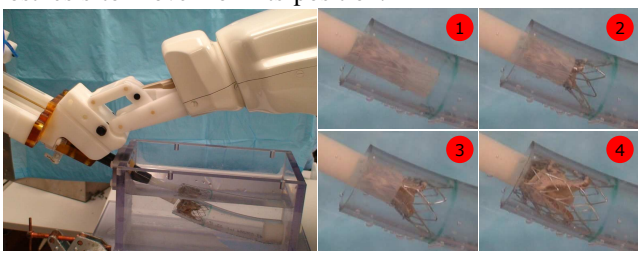

Fig. 5. (a) Experimental setup to test delivery module (b) Sequence of images showing the deployment of self-expanding prosthesis

V. Conclusion

Transapical aortic valve replacement is a minimally invasive procedure to implant a prosthetic valve via the apex of the beating heart. We present a robotic assisted system that allows for precise manipulation of cardiac interventional tools by a physician while he/she receives visual feedback from the real-time MR. A robotic value delivery module that can deploy both self-expanding and balloon-expandable stented prostheses was presented. The accuracy and repeatability of a redesigned valve delivery module was reported. In the preliminary ex-vivo phantom experiments, we observed that self-expanding prosthesis has a smaller positional error during deployment when using our robotic module.

A cooperative interface was used for the preparatory stage, whereas, image guidance was used to place the delivery module at the pre-planned trajectory. Finally, GUI along with real-time MRI feedback was used to localize and deploy the prosthesis. The smoothness, speed and error of the pneumatically actuated valve delivery module was tested. The smoothness and speed are important factors in the interactive mode when the physician requires a quick response to start/stop/resume commands in order to adjust the position and orientation of the prosthesis. The position and velocity error of the combined motion of translation and insertion joints determine the accuracy of deployment of self-expanding prosthesis. The position and velocity error for all motions was less than 0.5 mm and 0.5 mm/s, respectively. We use a new compact fiducial that can be placed close to the volume of interest while the patient is on the MRI table. Our results show that this compact fiducial leads to a registration accuracy that is comparable to the larger multi-spherical marker registration method.

Preliminary results in ex-vivo experimentation shows that the robotic system provides sufficient capabilities for placing a bioprosthetic aortic valve using either balloon-expandable or self-expanding stents inside a beating heart under MRI guidance and can be translated into animal and clinical models.

Acknowledgement

This research was supported by the Intramural Research Program of the National Institutes of Health (NIH), National Heart, Lung, and Blood Institute and Clinical Center.

References

[1] S. V. Lichtenstein, A. Cheung, J. Ye, C. Thompson, R. Carere, S. Pasupati, and J. Webb, "Trasapical transcatheter aortic valve implantation in humans: initial clinical experience," *Circulation*, vol. 114, pp. 533–535, 2006.

[2] K. Horvath, M. Guttman, M. Li, R. Lederman, D. mazilu, O. Kocaturk, P. Karmarkar, T. Hunt, S. Kozlov, and E. McVeigh, "Beating heart aortic valve replacement using real-time mri guidance," *Innovations*, vol. 2, pp. 51–55, 2007.

[3] M. Li, D. Mazilu, and K. Horvath, "A mri compatible robotic delivery module for transapical aortic valve replacement," in *Int J Comput Assist Radiol Surg*, vol. 3(suppl1), 2008, pp. S82–83.

[4] M. Li, D. Mazilu, and K. A. Horvath, "Robotic system for transapical aortic valve replacement with mri guidance," in *Med. Image Comput. Comput. Assist. Interv.*, 2008, pp. 476–484.

[5] D. Mazilu, M. Li, A. Kapoor, and K. Horvath, "Robotically assisted minimally invasive aortic valve replacement under mri guidance," in *Int J Comput Assist Radiol Surg*, vol. 4(suppl1), 2009, pp. S89–09.

[6] A. Kapoor, B. Wood, D. Mazilu, K. A. Horvath, and M. Li, "Mr-compatible hands-on cooperative control of a pneumatically actuated robot," in *Proc. IEEE ICRA*, 2009, pp. 2681–2686.

[7] E. Grube, J. Laborde, B. Zickmann, U. Gerckens, T. Felderhoff, B. Sauren, A. Bootsveld, L. Buellesfeld, and S. Iversen, "First report on a human percutaneous transluminal implantation of a self-expanding valve prosthesis for interventional treatment of aortic valve stenosis," *Catheterization and Cardiovascular Interventions*, vol. 66, pp. 465–469, 2005.

[8] C. Huber, L. Cohn, and L. von Segesser, "First report on a human percutaneous transluminal implantation of a self-expanding valve prosthesis for interventional treatment of aortic valve stenosis," *J. Am. Coll. Cardiol.*, vol. 46, pp. 366–370, 2005.

[9] A. Krieger, R. Susil, C. Menard, J. Coleman, G. Fichtinger, E. Atalar, and L. Whitcomb, "Design of a novel mri compatible manipulator for image-guided prostate interventions," *IEEE Trans. Biomed. Eng.*, vol. 52, pp. 306–313, 2005.

[10] A. Patriciu, D. Petrisor, M. Muntener, D. Mazilu, M. Schar, and D. Stoianovici, "Automatic brachytherapy seed placement under mri," *IEEE Trans. Biomed. Eng.*, vol. 54, pp. 1499–1506, 2007.

[11] S. DiMaio, E. Samset, G. Fischer, I. Iordachita, G. Fichtinger, F. Jolesz, and C. Tempany, "Dynamic mri scan plane control for passive tracking of instruments and devices," in *Med. Image Comput. Comput. Assist. Interv.*, 2007, pp. 50–58.

[12] K. Chinzei, N. Hata, F. Jolesz, and R. Kikinis, "Mr compatible surgical assist robot: system integration and preliminary feasibility study," in *Med. Image Comput. Comput. Assist. Interv.*, 2000, pp. 921–930.

[13] D. Stoianovici, D. Song, D. Petrisor, D. Ursu, D. Mazilu, M. Mutener, M. Schar, and A. Patriciu, ""mri stealth" robot for prostate interventions," *Minimally Invasive Therapy & Allied Technologies*, vol. 16, pp. 241–248, 2007.

[14] G. Fischer, I. Iordachita, C. Csoma, J. Tokuda, S. DiMaio, C. Tempany, N. Hata, and G. Fichtinger, "Mri-compatible pneumatic robot for transperineal prostate needle placement," *IEEE/ASME Trans. Mechatron*, vol. 13, pp. 295–305, 2008.

[15] R. Taylor, P. Jensen, L. Whitcomb, A. Barnes, R. Kumar, D. Stoianovici, P. Gupta, Z. Wang, E. deJuan, and L. Kavoussi, "A steady-hand robotic system for microsurgical augmentation," *Intl. J. Robot. Res.*, vol. 18, pp. 1201–1210, 1999.

[16] B. Davies, S. Harris, W. Lin, R. Hibberd, R. Middleton, and J. Cobb, "Active compliance in robotic surgery - the use of force control as a dynamic constraint," *Proc. Inst. Mech. Eng. H.*, vol. 211, pp. 285–292, 1997.

[17] R. Taylor, J. Funda, B. Eldridge, K. Gruben, D. LaRose, S. Gomory, M. Talamini, L. R. Kavoussi, and J. Anderson, "A telerobotic assistant for laparoscopic surgery," *IEEE Eng. Med. Biol. Mag.*, vol. 184, pp. 279–287, 1995.

[18] G. Hirzinger, M. Fischer, B. Brunner, R. Koeppe, M. Otter, M. Grebenstein, and I. Schafer, "Advances in robotics: The dlr experience," *Intl. J. Robot. Res.*, vol. 18, pp. 1064–1087, 1999.

[19] A. Kapoor, M. Li, and R. H. Taylor, "Constrained control for surgical assistant robots," in *Proc. IEEE ICRA*, 2006, pp. 231–236.

[20] M. Li, D. Mazilu, B. J. Wood, K. A. Horvath, and A. Kapoor, "A robotic assistant system for cardiac interventions under mri guidance," in *Proc. SPIE Medical Imaging*, 2010.